Metrologia

PAPER

Statistics for quantifying aging in time transfer system delays

To cite this article: T E Parker *et al* 2023 *Metrologia* **60** 065011

IOP Publishing | Bureau International des Poids et Mesures Metrologia

Metrologia **60** (2023) 065011 (6pp) https://doi.org/10.1088/1681-7575/ad088b

Statistics for quantifying aging in time transfer system delays

T E Parker*, **R C Brown** and **J A Sherman**

National Institute of Standards and Technology, Boulder, CO, United States of America

E-mail: tom.parker@nist.gov

Received 5 July 2023, revised 27 September 2023
Accepted for publication 31 October 2023
Published 10 November 2023

Abstract

Residual time delays in time transfer systems such as two-way satellite time and frequency transfer (TWSTFT), or GPS carrier phase (GPSCP) change over time. A double difference such as TWSTFT—GPSCP provides information on the changes in the relative time delays of the two systems. These changes are referred to as aging or time dispersion. A first difference statistic, RMS time interval error, $\mathrm{TIE}_{\mathrm{RMS}}$, provides the RMS time dispersion. The time deviation statistic (TDEV) or a variation on the Allan deviation (ADEV), referred to here as ADEVS, provide information on the nature of the random fluctuations in aging. This paper describes analytical and Monte Carlo techniques used to estimate the aging (time dispersion) from TDEV or ADEVS statistics, and finds that the aging can be more than a factor of four larger than TDEV or ADEVS. The use of ADEVS is recommended over TDEV since it is sensitive to time drift.

Keywords: time transfer system delays, time dispersion, aging, TDEV, ADEV

(Some figures may appear in colour only in the online journal)

1. Introduction

A number of National Metrology Laboratories now have multiple, independent, high stability time transfer links. Typically these are two-way satellite time and frequency transfer, TWSTFT, and GPS carrier phase, GPSCP, though a few also have optical links. With two independent time transfer systems a double difference of, for example, TWSTFT-GPSCP can be calculated that eliminates the clock instabilities and offset. Figure 1 shows 12 years of daily average double difference data between the National Institute of Standards and Technology, NIST, and the Physikalisch-Technische Bundesanstalt, PTB, in Germany. Specifically, it is TWSTFT—GPSCP for UTC (NIST)—UTC (PTB). The GPS carrier phase data is TAIPPP [1] from the Bureau International des Poids et Mesures. A few known large time steps and outliers have been removed from the double difference. This data should not be considered a rigorous example of either fully calibrated or uncalibrated links. It is a mixture of both due to incomplete documentation at NIST in the early days of GPSCP. For the purposes of this study it is just an example of a long series of reasonably well behaved double difference data that includes some bridging calibrations on the TWSTFT and some small calibration steps in the recent GPSCP data.

Double difference data can provide valuable information on the long-term stability of time transfer systems, though it is the combined instabilities of both systems. Figure 2 shows the time deviation, TDEV, of the data in figure 1, where τ is the averaging time interval in seconds. Note that the last four points use TOTAL TDEV [2] to provide better confidence limits. TDEV is used here to characterize the noise type in this double difference data. We see from a weighted fit that the noise characteristic has a power law dependence of $\tau^{0.27}$, which is about half way between flicker phase, with no dependence on τ, and random walk phase (white frequency), which has a $\tau^{0.5}$ dependence.

2. Aging in time transfer systems

An important characteristic of time transfer systems is how the time delays through the systems change with time. This time dispersion [3] is sometimes referred to as aging [4]. The RMS time dispersion, d_{RMS}, can be calculated with a first difference statistic as shown in equation (1),

* Author to whom any correspondence should be addressed.

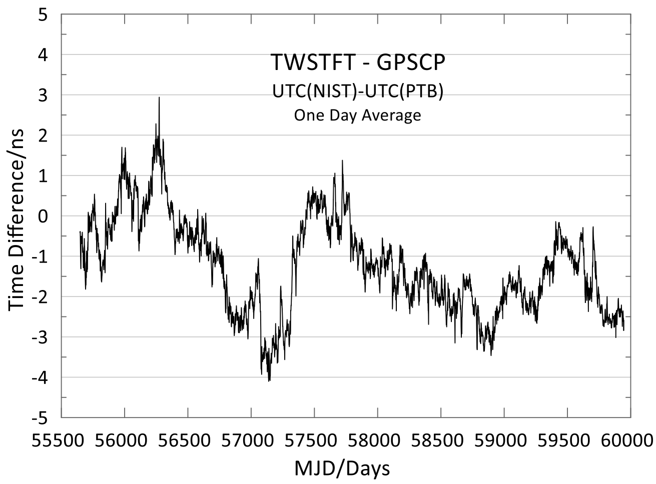

Figure 1. Double difference, TWSTFT—GPSCP, for UTC (NIST)—UTC (PTB). MJD is the modified Julian date.

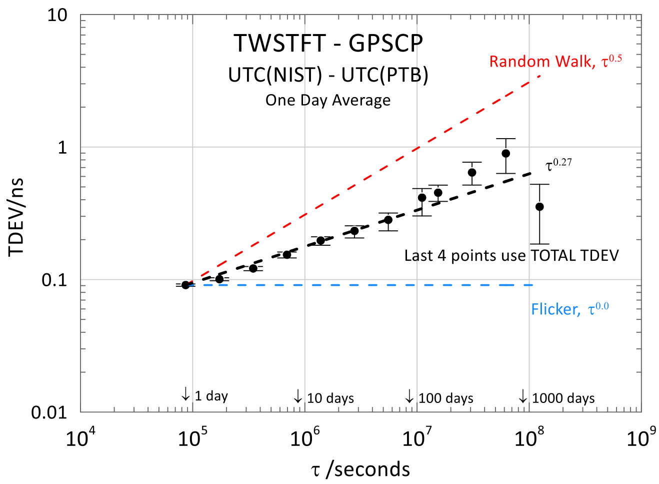

Figure 2. TDEV of data in figure 1. Dashed lines show various power law dependencies.

$$d_{\mathrm{RMS}}\left(\tau\right)=\sqrt{\frac{1}{n}\sum_{i=1}^{n}\left(d_{i+\tau}-d_{i}\right)^{2}} \qquad (1)$$

where d_i is the time difference at point i as in figure 1 and n is the number of data intervals. d_{RMS} is equivalent to the RMS time interval error, $\mathrm{TIE_{RMS}}$ in [5] which is used in the telecommunications industry. Time dispersion is quantified by d_{RMS}, but this statistic does not clearly distinguish noise types. Also, (1) can only be used on double difference data in which clock frequency offsets and clock instabilities have been removed by the differencing. Any apparent linear time drift (average frequency offset) in double difference data reflects a true change in time transfer delays and is a real contributor to aging.

A double difference and the commonly used TDEV provide valuable information on the magnitude and nature of aging. However, TDEV has an important weakness. As a second difference statistic on time it is insensitive to a linear drift in time. An alternative statistic to TDEV that does not have this problem is also available, though less commonly used. As shown in [6], the standard equation for the Allan deviation, ADEV, calculated from fractional frequency, y, can also be used with other parameters such as current or voltage, where y is replaced with another parameter. The same process can be used with double difference data, d, in which d_i is substituted for y_i. In this paper we will refer to this as ADEVS (S for substitute), to distinguish this statistic from the normal ADEV second difference calculation using time difference data. Like TDEV, ADEVS also distinguishes between white phase modulation, WPM, flicker phase modulation, FPM, and random walk phase modulation, RWPM, but also has the advantage that it is sensitive to time drift. The use of ADEVS in this study is discussed in section 2.2.

Time dispersion, or aging, can be calculated from (1) when the time series is available. However, the ability to determine time dispersion from TDEV, or ADEVS, can be important in situations where these statistics are available, but the corresponding time series is not, as in a three-corner-hat analysis [7] or a plot in a publication. The magnitude of the time dispersion is always larger than TDEV, or ADEVS, possibly by more than a factor of 4.

2.1. Analysis using TDEV

Because an analytical relation exists between TDEV and time dispersion for RWPM [3, 8], we will consider TDEV first in this section. Unfortunately, there is no analytical method to calculate time dispersion from TDEV for FPM, or intermediate processes between FPM and RWPM.

A Monte Carlo analysis was performed to provide information on the relation between time dispersion and TDEV for instabilities ranging from FPM to RWPM. The Allan Tools library developed for Python [9] was used to simulate FPM and RWPM phase noise in a time series. For FPM, the Allan Tools library function is based on a recursive summation of many white Gaussian noise processes with logarithmically distributed persistences. However, it does not generate power law dependencies between FPM and RWPM. To simulate noise with power laws between FPM, $\tau^{0.0}$, and RWPM, $\tau^{0.5}$, the method of Kasdin and Walter [10] was used. This method, based on computing the inverse Fourier transform of any spectral noise density of the form $S_y(f)\propto f^{\alpha}$, also computes and inserts a random phase noise series to make successive synthesized noises independent. However, especially over short averaging intervals, the Allan Tools simulator is more effective at generating pure FPM than the Kasdin method.

Each generated series has 500 000 data points and was repeated 100 times. The time dispersion, d, for the simulations is analogous to the time difference in figure 1. Figure 3 shows TDEV and RMS time dispersion, d_{RMS}, from the Allan Tools simulation of FPM and RWPM as a function of τ/τ_0, where τ_0 is the minimum averaging time. Error bars for d_{RMS} (derived from scatter in the 100 simulations) and TDEV are shown and are negligibly small. The heavy solid RWPM line is the analytical solution for d_{RMS} and the solid diamonds are

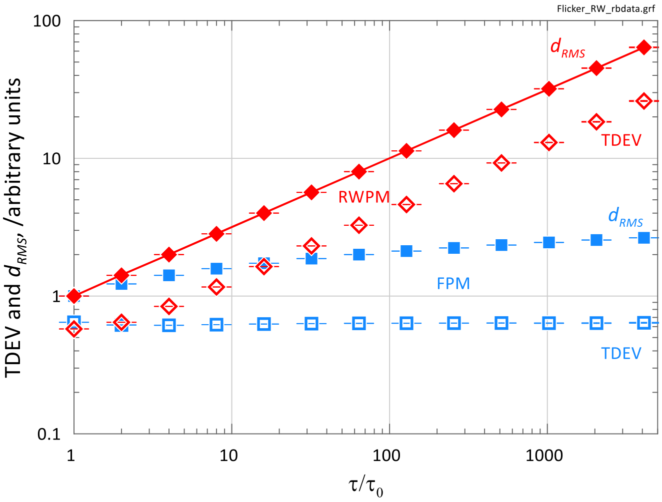

Figure 3. TDEV (empty) and RMS time dispersion, d_{RMS} (solid) from simulated FPM (squares) and RWPM (diamonds) data. The heavy solid red line is the analytical solution for RWPM based on TDEV.

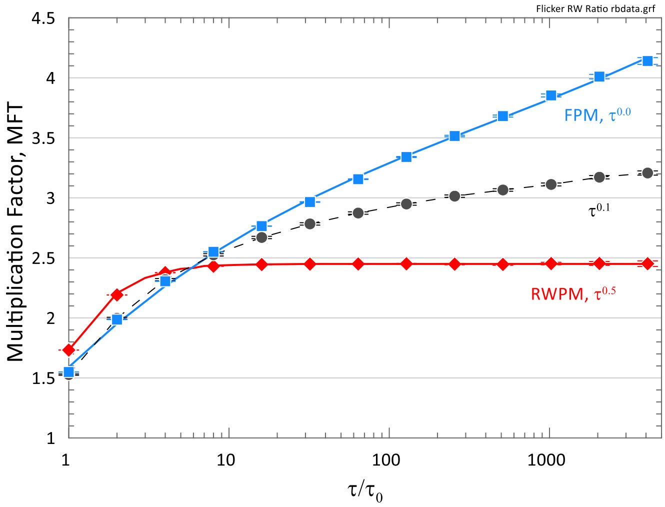

Figure 4. Multiplication factors from simulations of FPM (solid squares) and RWPM (solid diamonds). The solid lines represent a third order fit for FPM and the analytical solution for RWPM. An intermediate power law dependence of $\tau^{0.1}$ (solid dots) is also shown.

from the Monte Carlo analysis. The analytical expression for RWPM time dispersion, $d_{\mathrm{RMS},}$ is

$$d_{\mathrm{RMS(RWPM)}}(\tau) = \tau \times \sigma_y(\tau) \tag{2}$$

where $\sigma_y(\tau)$ is the Allan deviation, ADEV [3]. Using the relation between ADEV, and the modified Allan deviation, MDEV [8], and between MDEV and TDEV [11], we get

$$d_{\mathrm{RMS(RWPM)}}(\tau) = \sqrt{2}\sqrt{3}\mathrm{TDEV}(\tau) = 2.45\mathrm{TDEV}(\tau) \tag{3}$$

for $\tau/\tau_0 > 10$. Here τ_0 can be viewed as 1 d in figure 3, to be consistent with figure 1. For $\tau/\tau_0 < 10$, see the numerical values in [8]. The agreement is very good between the RWPM analytical and simulated methods and confirms the validity of the Monte Carlo analysis. The solid squares and the empty squares show the results for FPM instabilities. Note that d_{RMS} is larger than TDEV for both FPM and RWPM instabilities.

The ratio of d_{RMS} over TDEV will be defined as the multiplication factor, MFT, such that

$$d_{\mathrm{RMS}}(\tau) \equiv \mathrm{MFT}(\tau) \times \mathrm{TDEV}(\tau). \tag{4}$$

Figure 4 shows MFT for FPM and RWPM instabilities for intervals from 1 to 4000 from the data in figure 3. Again, the solid RWPM line represents the analytical solution and is in good agreement with the simulated results [12]. From (3) we see that MFT for RWPM equals 2.45 for $\tau/\tau_0 > 10$. The intermediate line (solid dots) also shown is discussed below.

The solid FPM line in figure 4 is a third order fit to the simulated data. Here we see that MFT ranges from 1.5 to about 4.2. The third order fit equation is:

$$\mathrm{MFT_{FPM}} = 1.590 + 1.283\mathrm{Log}(\tau) - 0.2892(\mathrm{Log}(\tau))^2 + 0.0364(\mathrm{Log}(\tau))^3. \tag{5}$$

TDEV for FPM noise is dependent on the measurement bandwidth, f_h, in the term $\omega_h\tau_0$, where $\omega_h = 2\pi f_h$ in [8]. From the ratio of MDEV/ADEV for the Allan Tools simulated FPM, we find that the effective bandwidth parameter is $\omega_h\tau_0 \cong 3$ [8]. See below for more discussion of bandwidth.

To simulate noise with power law dependencies between FPM, $\tau^{0.0}$ and RWPM, $\tau^{0.5}$, the Kasdin method was used. For FPM it does not generate as flat a TDEV characteristic as the Allan Tools simulator, but MFTs for the two techniques agree to within 4%. The MFT agreement between Kasdin and Allan Tools for RWPM is very good at better than 0.1%. The solid dots in figure 4 show MFT for $\tau^{0.1}$, illustrating that MFT changes rapidly in going from FPM to RWPM. The effective bandwidth parameter, $\omega_h\tau_0$, for Kasdin FPM is midway between 3 and 10, making it a little larger than with Allan Tools FPM. The effective bandwidth is important in experimental data and is dependent on the amount of averaging. For example, in figure 1 it is a one day average. This will have a small affect on MFT. The fact that it is different for Kasdin and Allan Tools simulations reflects the different techniques used to produce the simulations.

Figure 5 shows MFT calculated using the Kasdin model as a function of the TDEV power law exponent x, (as in τ^x), for x ranging from 0 to 0.5. Curves for various τ values relevant to aging for $\tau/\tau_0 > 10$ are shown. The data in figure 5 show that MFT $\sim$ 2.5 for $0.25 < x \leqslant 0.5$ and $\tau/\tau_0 > 10$. MFT is larger and depends strongly on x and τ/τ_0 for x below $\sim$0.25. Table 1 shows the MFT values and uncertainties from figure 5.

2.2. Analysis using ADEVS

Following the same procedures as in section 2.1, the multiplication factor has been calculated using ADEVS. As mentioned above, ADEVS was calculated by replacing y_i with d_i in the standard equation for ADEV using fractional frequency

Table 1. Values of MFT and uncertainties in figure 5.

	$\tau/\tau_0 = 16$		$\tau/\tau_0 = 128$		$\tau/\tau_0 = 1024$		$\tau/\tau_0 = 8192$	
x	MFT	Unc.	MFT	Unc.	MFT	Unc.	MFT	Unc.
0.00	2.894	0.012	3.482	0.014	3.973	0.019	4.405	0.033
0.05	2.771	0.011	3.182	0.012	3.466	0.015	3.671	0.028
0.10	2.670	0.010	2.949	0.010	3.112	0.012	3.257	0.023
0.15	2.589	0.009	2.774	0.009	2.873	0.011	2.926	0.023
0.20	2.522	0.008	2.646	0.008	2.694	0.009	2.722	0.021
0.25	2.473	0.008	2.551	0.007	2.572	0.008	2.592	0.019
0.30	2.438	0.007	2.487	0.006	2.501	0.007	2.501	0.018
0.35	2.419	0.007	2.447	0.005	2.454	0.007	2.446	0.020
0.40	2.412	0.007	2.428	0.005	2.436	0.007	2.424	0.019
0.45	2.421	0.006	2.430	0.005	2.426	0.008	2.438	0.019
0.50	2.445	0.006	2.450	0.004	2.451	0.007	2.442	0.021

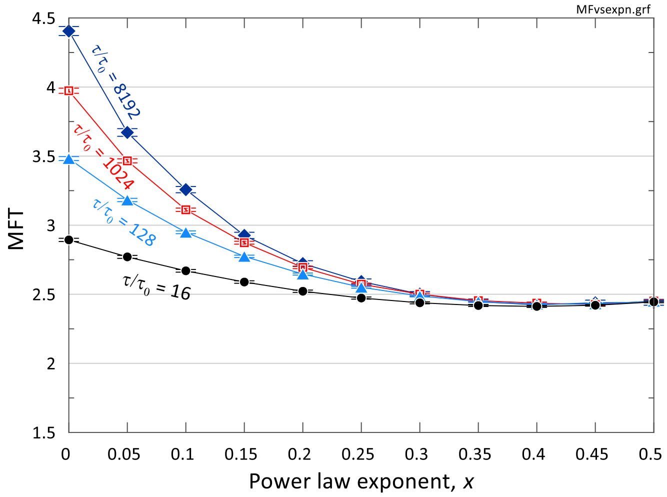

Figure 5. MFT for various τ/τ_0 values as a function of the TDEV power law dependence, x.

y_i. ADEVS has the same power law dependence as TDEV for the various PM noise types but is sensitive to a linear drift in time difference. ADEVS is about 10% larger than TDEV for FPM and about 39% larger for RWPM. The multiplication factor using ADEVS, MFA, is defined in a manner analogous to MFT as shown below,

$$d_{\mathrm{RMS}}(\tau) \equiv \mathrm{MFA}(\tau) \times \mathrm{ADEVS}(\tau). \qquad (6)$$

Figure 6 shows MFA as a function of τ/τ_0 for $x = 0$ (FPM), $x = 0.1$, and $x = 0.5$ (RWPM) and is similar to figure 4. We see that MFA is 1.4 at $\tau/\tau_0 = 0$ for all three values of x, and is a constant value of 1.73 for RWPM at $\tau/\tau_0 > 10$. For FPM, MFA approaches 4 at large τ/τ_0. MFA is overall smaller than MFT. Figure 7 shows the results for the power law dependence of MFA and is analogues to figure 5 for MFT. Table 2 shows the values of MFA and the uncertainties from figure 7.

Simulated data shows that MFA = 1.41 in the limit where drift dominates over random fluctuations. Because ADEVS is sensitive to drift, the use of ADEVS is recommended over TDEV.

3. Discussion

For the simulated FPM and RWPM data there is always a small linear drift component (the first and last data points are never the same). However, it has no significant impact on the results of this study. At $\tau/\tau_0 = 4096$, ADEVS is reduced by less than 2% for both FPM and RWPM when the drift is removed from the data set. The reduction is even smaller at smaller τ/τ_0.

Figure 8 shows d_{RMS} calculated from the data in figure 1 using (1), and d_{RMS} estimated from MFT and TDEV in figure 2, where $x \sim 0.27$. A similar plot using MFA and ADEVS is also shown. Error bars are not available for the calculated d_{RMS}. The agreement with d_{RMS} is very good for both TDEV and ADEVS, illustrating that the method works well on this real data. TDEV can be used here because the average drift (-0.5 ps d^{-1}) in figure 1 is small compared to the level of random fluctuations. Removing the average drift has a negligible impact on the results, with d_{RMS} reduced by only 4.5% at $\tau = 1024$ d, and less at smaller τ values. The estimate of $\omega_h\tau_0$ for the TWSTFT—GPSCP double difference data is close to 3.

When calibrating time transfer systems it is important to know how fast the calibration uncertainty will degrade over

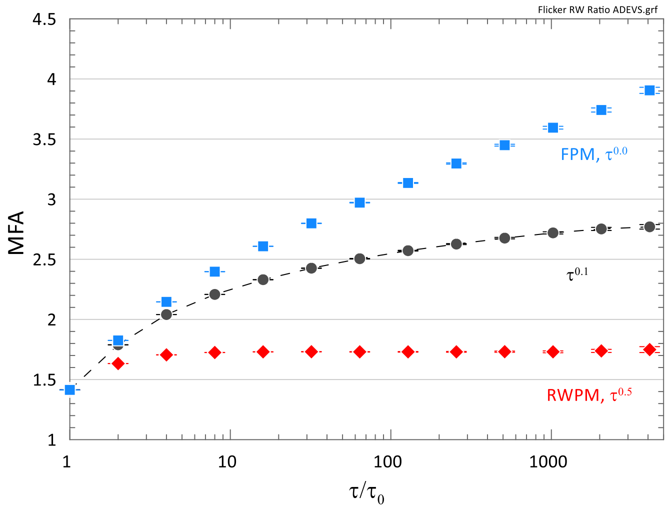

Figure 6. Multiplication factors, MFA, from simulations of FPM (solid squares) and RWPM (solid diamonds). An intermediate power law dependence of $\tau^{0.1}$ (solid dots) is also shown.

Table 2. Values of MFA and uncertainties in figure 7.

	$\tau/\tau_0 = 16$		$\tau/\tau_0 = 128$		$\tau/\tau_0 = 1024$		$\tau/\tau_0 = 8192$	
x	MFA	Unc.	MFA	Unc.	MFA	Unc.	MFA	Unc.
0.00	2.608	0.001	3.135	0.004	3.595	0.012	4.039	0.037
0.05	2.461	0.001	2.820	0.003	3.090	0.010	3.310	0.031
0.10	2.330	0.001	2.572	0.003	2.720	0.009	2.813	0.028
0.15	2.218	0.001	2.377	0.003	2.439	0.008	2.479	0.026
0.20	2.118	0.001	2.220	0.003	2.261	0.008	2.298	0.025
0.25	2.033	0.001	2.102	0.003	2.125	0.008	2.116	0.024
0.30	1.957	0.001	1.994	0.002	2.003	0.007	2.016	0.027
0.35	1.890	0.001	1.911	0.002	1.915	0.007	1.917	0.029
0.40	1.830	0.001	1.840	0.002	1.846	0.007	1.857	0.037
0.45	1.777	0.001	1.783	0.002	1.785	0.007	1.783	0.036
0.50	1.730	0.001	1.730	0.002	1.731	0.008	1.765	0.054

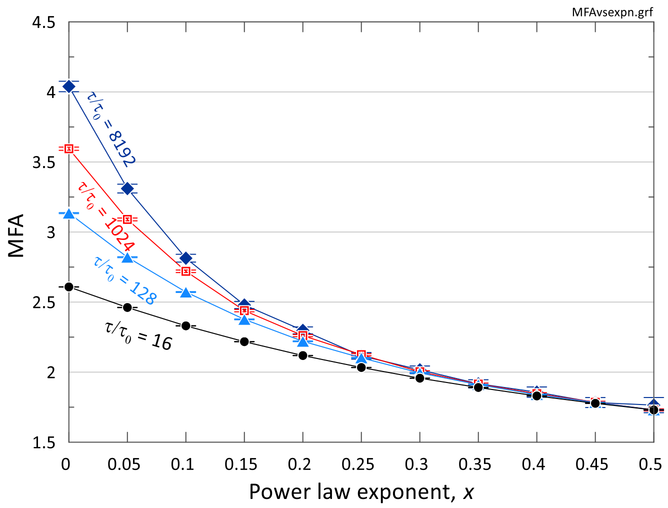

Figure 7. MFA for various τ/τ_0 values as a function of the ADEVS power law dependence, x.

time, or age. If double difference data is available, an estimate can be made based on the analysis in this paper. Of course the double difference data does not provide information on the individual systems, but estimates can be made. A conservative estimate would be to assume all the aging is in the system of interest. Based on a three corner hat analysis of

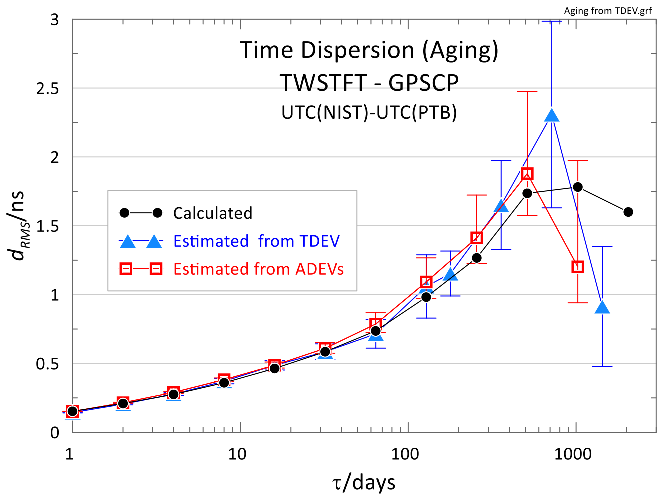

Figure 8. Calculated and estimated time dispersion, d_{RMS}, for data in figure 1.

time transfer instabilities [6], a more reasonable estimate for TWSTFT—GPSCP is to divide the double difference TDEV by $\sqrt{2}$ under the assumption that the levels of instabilities are similar. However, there is some risk of underestimating the level of aging with this approach.

Tables 1 and 2 can be used as guidelines for estimating d_{RMS} over time frames relevant to aging if only TDEV or ADEVS are available. Multiplication factors range from 1.7 to more than 4 when noise processes in the range from FPM to RWPM dominate. White phase noise, $x = -0.5$, is generally not present in the time range relevant to aging [7]. For the noise processes that are commonly observed in aging the multiplication factors tend to be in the lower range around 2.

4. Summary

When double difference data is available from time transfer systems, the time dispersion, d_{RMS}, can be calculated using $\mathrm{TIE}_{\mathrm{RMS}}$, which is available in Python Allan Tools [9] and Stable32 [13]. This provides valuable information on the aging of time delays in transfer systems. If double difference data is not available, we have shown that d_{RMS}, can be estimated from TDEV or ADEVS, when the nature of the instabilities falls in the range from flicker phase to random walk phase. ADEVS can be used in the presence of significant drift. For random fluctuations the time dispersion is always larger than TDEV or ADEVS, and the multiplication factor ranges from 1.73 to more than 4 for FPM at large τ. Though the use of TDEV is more common, it is recommended that ADEVS be used to characterize time transfer instabilities since it is sensitive to drift, whereas TDEV is not.

Acknowledgments

The authors thank our colleagues at PTB for the TWSTFT and GPSCP data, and also acknowledge valuable discussions with Judah Levine and Biju Patla.

ORCID iDs

T E Parker https://orcid.org/0000-0003-3264-9245
R C Brown https://orcid.org/0000-0002-8228-4283
J A Sherman https://orcid.org/0000-0002-8560-481X

References

[1] Petit G and Jiang Z 2008 Precise point positioning for TAI computation *IJNO 2008* pp 1–8
[2] Weiss M and Howe D Total TDEV *Proc. 1998 IEEE Int. Frequency Control Symp.* pp 192–8
[3] Allan D 1987 Time and frequency (time-domain) characterization, estimation, and prediction of precision clocks and oscillators *IEEE Trans. Ultrason. Ferroelectr. Freq. Control* **34** 647–54
[4] Jiang Z *et al* 2011 BIPM calibration scheme for UTC time links *Proc. 2011 Joint Conf. of the IEEE Int. Frequency Control Symp. and the European Frequency and Time Forum* pp 1–6
[5] Riley W 2008 *Handbook of Frequency Stability Analysis* vol 1065 (NIST Special Publication) p 34
[6] Rubiola E, Francese C and de Marchi A 2001 Long-term behavior of operational amplifiers *IEEE Trans. Instrum. Meas.* **50** 89–94
[7] Parker T, Zhang V, Petit G, Yao J, Brown R C and Hanssen J L 2022 A three-cornered hat analysis of instabilities in two-way and GPS carrier phase time transfer systems *Metrologia* **59** 035007
[8] Sullivan D, Allan D, Howe D and Walls F 1990 Characterization of clocks and oscillator *NIST Technical Note 1337* pp TN9–TN12
[9] Wallin A E E*et al* 2019 *Allantools* (available at: https://github.com/aewallin/allantools)
[10] Kasdin N and Walter T 1992 Discrete simulation of power law noise *Proc. 1992 IEEE Frequency Control Symp.* pp 274–83
[11] Allan D, Weiss M and Jespersen J 1991 A frequency-domain view of time-domain characterization of clocks and time and frequency distribution systems *Proc. 45th Freq. Cont. Symp.* pp 667–78
[12] There is an asymptotic form for with FPM [3]. However, the region of validity is not well characterized for the averaging intervals of interest here
[13] Riley W 2020 *Stable32 Software* (available at: www.stable32.com)